

Coherent Single Photon Transport in a One-Dimensional Waveguide Coupled with Superconducting Quantum Bits

Jung-Tsung Shen and Shanhui Fan*

Ginzton Laboratory, Stanford University, Stanford, California 94305, USA

(Received 13 June 2005; published 14 November 2005)

A recent theoretical analysis [A. Blais *et al.*, Phys. Rev. A **69**, 062320 (2004)] and experimental results [A. Wallraff *et al.*, Nature (London) **431**, 162 (2004)] show that interesting transport properties of a single microwave photon emerge when a quantum bit in a cavity is coupled to a one-dimensional waveguide. Here we adopt a real-space model Hamiltonian to give a unified approach which accounts for the experimental results, and make new predictions on the properties of single photon transport, such as the general Fano line shape, symmetric vacuum Rabi splitting for a leaky cavity at resonance, and a one-photon switching capability.

DOI: [10.1103/PhysRevLett.95.213001](https://doi.org/10.1103/PhysRevLett.95.213001)

PACS numbers: 32.80.-t, 03.67.Lx, 42.50.-p, 74.50.+r

The studies of interactions of electromagnetic fields with two-level systems is of fundamental importance. One goal of these studies is to achieve the limit where a single two-level system couples strongly to a single photon to exhibit coherent behavior, which has been a main theme of quantum optics of the past two decades and has generated the field of cavity quantum electrodynamics (cavity QED) [1,2]. In a recent theoretical proposal [3] and an experimental report [4], the strong coupling is achieved by embedding a Cooper pair box in a resonator capacitively coupled to a one-dimensional microwave transmission line waveguide (coplanar waveguide), as shown in Fig. 1(a). In a transmission line waveguide, the photon state forms a one-dimensional continuum, and accordingly, the experimental setup in Ref. [4] probes the couplings between the Cooper pair box, the resonator, and the one-dimensional waveguide modes.

In this Letter, we point out some of the important consequences resulting from coupling to the one-dimensional continuum. The spontaneous emission of the excited two-level system, as well as the mode leakage of the cavity, i.e., the interactions of the system with the external environment is generally treated as a loss and decoherence mechanism and is included as part of the absorption coefficient or decay rate of the system [5]. Contrary to this, it has been shown recently that when the two-level systems, with or without a cavity (resonator), are coupled with a one-dimensional continuum, the spontaneous emission from two-level systems and the leaked waves out of the cavity, can coherently interfere with the propagating modes in the one-dimensional continuum, and results in interesting transport properties [6]. Here, we adopt this method to give a unified and fully quantum mechanical approach to model the recent Cooper pair box experiment, and make predictions about the transport properties of the photons which can be verified by further experiments.

The Cooper pair box, a mesoscopic superconducting island connected to a large reservoir via Josephson junction, can form a quantum bit (qubit) with two states in the

charge regime with suitable gate voltage [7–9]. In this regime, the Hamiltonian describing the Cooper pair box is

$$H = \sum_n 4E_C(n - n_g)^2 |n\rangle\langle n| - \frac{1}{2} E_J (|n\rangle\langle n+1| + |n+1\rangle\langle n|), \quad (1)$$

where E_C is the charging energy, E_J is the Josephson coupling energy, n is the excess Cooper pair number on the island, and n_g is the tunable dimensionless gate charge [3,10]. The two eigenstates of the qubit, denoted by $|-\rangle$ and $|+\rangle$, are obtained by diagonalizing Eq. (1) for $n = 0$ and 1. The Cooper pair box has advantages of long coherence time [7,8] and large effective electric dipole moment [3], which makes it especially well suited to reach the strong coupling limit in cavity QED. If two parallel Josephson junctions are used to connect the Cooper pair box to form a SQUID loop, the Josephson coupling energy, $E_J = E_J^{\max} |\cos(\pi\phi/\phi_0)|$, can be controlled by threading the loop with a magnetic flux ϕ (where $\phi_0 = h/2e$ is the flux quantum). The transition energy Ω between the two eigenstates is $\Omega = \sqrt{E_J^2 + 16E_C^2(1 - 2n_g)^2}$. Ω is equal to E_J when $n_g = 1/2$, i.e., at the degeneracy point [8].

The interaction between the Cooper pair box (qubit), and the propagating multimode photons is described by the Dicke Hamiltonian [11]:

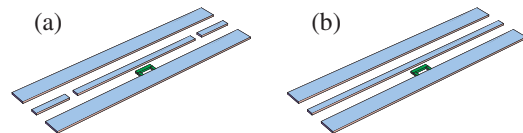


FIG. 1 (color online). Schematics of the systems. (a) A Cooper pair box is embedded in a cavity coupled to a one-dimensional transmission line waveguide. The three horizontal bars indicate the waveguide. The cavity is formed by two capacitive open gaps in the center line. (b) Without cavity.

$$H = \frac{1}{2}\hbar\Omega\sigma_z + \sum_k \hbar\omega_k a_k^\dagger a_k + \sum_k V_k (a_k^\dagger + a_k)(\sigma_+ + \sigma_-), \quad (2)$$

where the first term describes the two eigenstates $|-\rangle$ and $|+\rangle$ of an isolated Cooper pair box, Ω is the transition energy; the second term represents the energy of the propagating photons, ω_k is the frequency (i.e., dispersion relation) of the photon with wave vector (i.e., mode index) k , and $a_k^\dagger(a_k)$ is the bosonic creation (annihilation) operator of the photon; the third term describes the interaction; $V_k = (2\pi\hbar/\omega_k)^{1/2}\mathbf{\Omega}\mathbf{D}\cdot\mathbf{e}_k$ is the coupling between the photons and the qubits. \mathbf{D} is the dipole moment of the Cooper pair box, \mathbf{e}_k is the polarization unit vector of the photon. $\sigma_+ = a_e^\dagger a_g$ and $\sigma_- = a_g^\dagger a_e$ are the usual ladder operators that change the state of the qubit and satisfy $\sigma_+|-\rangle = |+\rangle$ and $\sigma_+|+\rangle = 0$. $a_g^\dagger(a_e^\dagger)$ is the fermionic creation operator of the $|-\rangle(|+\rangle)$ state of the qubit.

In one dimension, when the resonance energy of the two-level system is away from the cutoff frequency of the dispersion relation, we rewrite the Hamiltonian of the system in real space as

$$H = \int dx \left\{ -iv_g c_R^\dagger(x) \frac{\partial}{\partial x} c_R(x) + iv_g c_L^\dagger(x) \frac{\partial}{\partial x} c_L(x) + V\delta(x)(c_R^\dagger(x)\sigma_- + c_R(x)\sigma_+ + c_L^\dagger(x)\sigma_- + c_L(x)\sigma_+) \right\} + E_e a_e^\dagger a_e + E_g a_g^\dagger a_g, \quad (3)$$

where v_g is the group velocity of the photons, and $c_R^\dagger(x)(c_L^\dagger(x))$ is a bosonic operator creating a right-going (left-going) photon at x . $E_e - E_g (\equiv \Omega)$ is the transition energy. In deriving Eq. (3), we assume the dispersion relations are nondegenerate, linearize the dispersion relation of the photons in the waveguide, and replace V_k by a constant V . This Hamiltonian is similar to the Anderson $s-d$ model in condensed matter physics, which describes the S -wave scattering of electrons off a magnetic impurity in three dimensions [12,13]. A similar one-mode Hamiltonian has also been investigated [14].

We first highlight the physics of the coherent interference in the waveguide geometry. Consider two-level systems coupled to a one-dimensional continuum [Fig. 1(b)]. In this case, the excited two-level system will decay exponentially. However, in the reduced dimensionality, when a single photon is incident upon the two-level system with a frequency on resonance, the wave function of the spontaneously emitted photon inevitably interferes coherently with that of the incident wave, due to the forward and backward directions being the only directions in phase space. Such interference can result in the photon being completely reflected with no loss. This occurs in spite of the fact that the physical dimension of the two-level system is typically far smaller than the wavelength of light. Thus spontaneous emission can be exploited to influence the coherent transport properties of a single photon.

In one-dimensional scattering, for a single photon, the most general line shapes of the transmission and reflection spectra are of the Fano type [15]. The Fano line shape is asymmetric and is completely specified by two phase shifts passing through the scatterer and the environment. These two phase shifts correspond to the direct and the resonance-assisted indirect pathways, respectively [16], and the interference between these two phase shifts results in the Fano line shape of the transmission spectrum [15]. When the scattering potential possesses parity symmetry, the transmission amplitude is given by $t = 1/2(e^{2i\delta_0(E)} + e^{2i\delta_1(E)})$, where $\delta_0(E)$ and $\delta_1(E)$ are the phase shift of the even and odd wave, respectively, and E is the energy of the photon. The transmission coefficient is given by $T \equiv |t|^2 = \cos^2(\delta_0 - \delta_1)$.

For the short-ranged potential, $kU \ll 1$ (k is the momentum of the photon, and U denotes the range of the potential, which is roughly the size of the two-level system), $\delta_1 \equiv 0$ by symmetry. In general, there are two contributions to $\delta_0(E)$: one from the scatterer, and one from the background, and only the background contributes to $\delta_1(E)$. δ_0 takes the form $\delta_0(E) = \delta_{\text{res}}(E) + \delta_{bg,0}(E)$, and $\delta_1(E) = \delta_{bg,1}(E)$. $\delta_{\text{res}}(E) = \arctan[\Gamma/2/(E - \Omega)]$, where Ω again is the resonant energy of the scatterer, and $\Gamma/2$ is the decay rate. The background phase shifts, $\delta_{bg,0}(E)$ and $\delta_{bg,1}(E)$, come from the environments where the two-level system is located, such as the embedding material, or the partially transmitting elements forming the cavity within the one-dimensional waveguide. This phase shift provides tunability of the transmission line shape. In the special case when $\delta_{bg} \equiv \delta_{bg,0}(E) - \delta_{bg,1}(E)$ is 0, which corresponds to the cases shown in Fig. 1(b), the transmission profile is (anti-) Lorentzian, and has a dip down to 0 at resonance energy Ω . The transmission line shape can be completely inverted when δ_{bg} is close to $\pi/2$, and exhibits asymmetric features when δ_{bg} takes values between 0 and $\pi/2$ [Fig. 1(a)].

Consider the optical system consisting of a two-level system embedded in a one-dimensional waveguide, as shown in Fig. 1(b). Assume a photon is coming from the left with energy $E_k = v_g k$. The stationary state of the system is

$$|E_k\rangle = \int dx \{ \phi_{k,R}^+(x) c_R^\dagger(x) + \phi_{k,L}^+(x) c_L^\dagger(x) \} |0, -\rangle + e_k a_e^\dagger a_g |0, -\rangle, \quad (4)$$

where $|0, -\rangle$ is the vacuum state with zero photon and the two-level system is unexcited, and e_k is the probability amplitude of the two-level system in the excited state. Equation (4) represents a complete basis for the system. For a photon incident from the left, $\phi_{k,R}^+(x)$ and $\phi_{k,L}^+(x)$ take the form

$$\begin{aligned} \phi_{k,R}^+(x) &\equiv (e^{ikx}\theta(-x) + te^{ikx}\theta(x)), \\ \phi_{k,L}^+(x) &\equiv re^{-ikx}\theta(-x), \end{aligned} \quad (5)$$

where t, r are the transmission and reflection amplitude, respectively.

From the eigenvalue equation $H|E_k\rangle = E_k|E_k\rangle$, together with the commutation relations, we obtain $t = \cos be^{ib}$, $r = i \sin be^{ib}$, $e_k = -(v_g/V)(\sin be^{ib})$, where the phase shift is $b = \arctan[V^2/(v_g(\Omega - E_k))]$.

The reflection coefficient is given by

$$R \equiv |r|^2 = \sin^2\left(\arctan\left(\frac{V^2}{v_g(\Omega - E_k)}\right)\right) = \frac{(V^2/v_g)^2}{(\Omega - E_k)^2 + (V^2/v_g)^2}, \quad (6)$$

which shows a Lorentzian line shape.

From t and r it follows that the transfer matrix for one two-level system has the following form:

$$\begin{pmatrix} a' \\ b' \end{pmatrix} = \begin{pmatrix} 1 - \frac{iV^2}{v_g(\Omega - E_k)} & -\frac{iV^2}{v_g(\Omega - E_k)} \\ +\frac{iV^2}{v_g(\Omega - E_k)} & 1 + \frac{iV^2}{v_g(\Omega - E_k)} \end{pmatrix} \begin{pmatrix} a \\ b \end{pmatrix}. \quad (7)$$

The transfer matrix relates the incoming and outgoing wave amplitudes $a(b')$ and $b(a')$ on both sides of the two-level system. Note the form of the transfer matrix is the same as when the waveguide is side coupled to a single-mode cavity [17–19].

Figure 2 shows a typical transmission and reflection spectrum. The line shape is a universal function of $(E_k - \Omega)/(V^2/v_g)$, and, consequently, the width is proportional to V^2/v_g . At resonance, the photon is completely reflected and the single two-level system behaves as a mirror. The notable feature of this result is that the spontaneous emission directly gives rise to the reflection, rather than losses that degrade the performance.

A more general Fano line shape can be created if there are partial reflections in the waveguide such that the photon modes are no longer purely forward or backward propagating. As an example, consider a case where the two-level system is surrounded by a pair of capacitive open gaps [Fig. 1(a)]. The presence of the partially reflecting elements introduces a background phase shift, in addition to the phase shift experienced by the photon due to the two-level system. The response function of the system can be

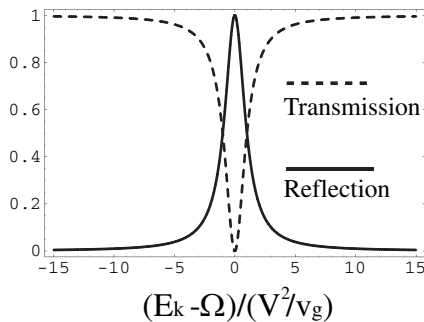


FIG. 2. The transmission spectrum (dashed line) and the reflection spectrum (solid line) for a two-level system in a one-dimensional waveguide as shown in Fig. 1(b).

calculated by combining the transfer matrix of each individual element in the system. The general form of the transfer matrix for any partially reflecting elements with time reversal symmetry is described by [20]

$$T_g = \begin{pmatrix} 1/\bar{t}^* & -\bar{r}^*/\bar{t}^* \\ -\bar{r}/\bar{t} & 1/\bar{t} \end{pmatrix}, \quad (13)$$

where \bar{t} and \bar{r} , satisfying $|\bar{t}|^2 + |\bar{r}|^2 = 1$, are the amplitudes of transmittance and reflectivity, respectively. The gaps act as potential barriers for the single photon, and are modeled by [21] $\bar{r} = r_{12}(1 - X^2)/(1 - r_{12}^2 X^2)$, where $r_{12} = (Z_2 - Z_1)/(Z_2 + Z_1)$ is the reflection amplitude at single interface of each gap. Z_1 and Z_2 are the impedances of the waveguide and the discontinuity, respectively. $0 \leq X \leq 1$ is a real number determined by the geometry of the gap. Having two gaps, as shown in Fig. 1(a), then creates a cavity (with a cavity resonance frequency ω_r).

The presence of the cavity spoils the transmission spectrum from being a universal function of $(E_k - \Omega)/(V^2/v_g)$, and the shape of the spectrum strongly depends on the value of \bar{r} , the qubit transition energy Ω , and the coupling strength V . Figure 3 shows the transmission spectrum of the total system for several different scenarios. When the Cooper pair box is in resonance with the resonator, the resonance peak splits and shows vacuum Rabi splitting, as shown in Fig. 3(a). From the transfer matrices, it can be rigorously shown that the splitting is always sym-

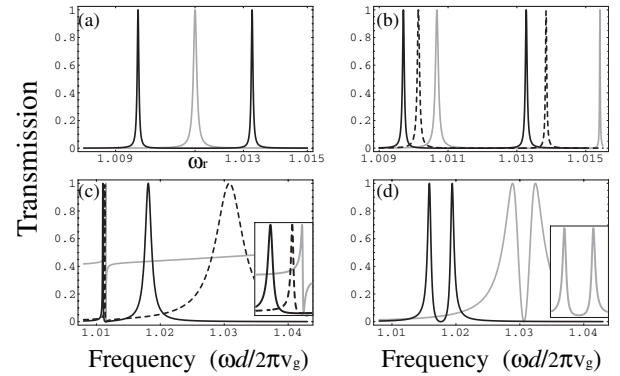


FIG. 3. The transmission spectra through the total system corresponding to Fig. 1(a). The frequency is in units of $\omega_0 \equiv 2\pi v_g/d$, $V^2/v_g = 10^{-5}\omega_0$, $Z_1 = 50$, and $Z_2 = -1500i$. (a) Gray line: the cavity mode without the Cooper pair box. The resonance peak is located at $\omega_r = 1.01148738\omega_0$. Solid line: vacuum Rabi splitting. The Cooper pair is in resonance with the cavity. $X = 0.2$ ($|\bar{r}| \approx 0.9996$). (b) Off resonance. Solid line: $\Omega = \omega_r$. Dashed line: $\Omega = 1.0125\omega_0$. Gray line: $\Omega = 1.0146\omega_0$. (c) Off resonance for leaky cavity. $\Omega = 1.01148738\omega_0$. Solid line: $X = 0.5$ ($|\bar{r}| \approx 0.996$). Dashed line: $X = 0.7$ ($|\bar{r}| \approx 0.984$). Gray line: $X = 0.96$ ($|\bar{r}| \approx 0.525$). Inset shows the details of the overlapping peaks at normalized frequency around 1.01. (d) On resonance (zero detuning) for the leaky cavity. Solid line: $\Omega = 1.017631\omega_0$, $X = 0.5$ ($|\bar{r}| \approx 0.996$). Gray line: $\Omega = 1.030651\omega_0$, $X = 0.7$ ($|\bar{r}| \approx 0.984$). Inset shows the case when the coupling is 5 times larger: $V^2/v_g = 25 \times 10^{-5}\omega_0$, $\Omega = 1.030651\omega_0$, $X = 0.7$.

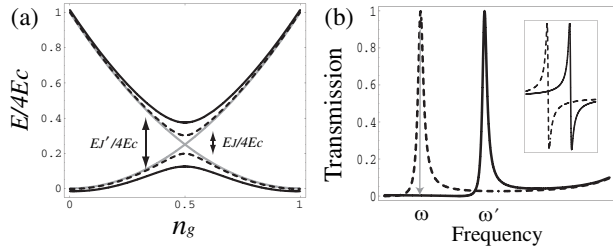


FIG. 4. One-photon switching. (a) Energy diagram of the single Cooper pair box. The dashed and the solid curves represent before and after the change of magnetic flux, respectively. The gray curve denotes the noninteracting case. $4E_c$ is adopted as the energy unit. (b) The transmission peaks for a qubit in a cavity coupled to the waveguide. The solid and dashed curves correspond to those in (a), respectively. The gray line denotes the change of transmission.

metric at resonance, even for a very leaky cavity. The splitting and the line shape, however, become asymmetric at off resonance. When the Cooper pair box is proceedingly detuned away from resonance, the two vacuum Rabi splitting peaks behave differently in the changes of the locations and the line shapes. Figure 3(b) shows the evolution of the two peaks when the Cooper pair box is brought away from resonance towards higher frequency ($\Delta \equiv \Omega - \omega_r > 0$). The high frequency peak moves away and narrows at a rate faster than the low frequency peak does. The case when $\Delta < 0$ behaves oppositely. Figure 3(c) shows the transmission spectrum for a leaky (low- Q) cavity at off resonance. The sharp Fano line shape becomes evident at large detuning [Fig. 3(c), inset]. Figure 3(d) shows the case of a low- Q cavity and zero detuning. The radiative rate of the Cooper pair box into the one-dimensional continuum is strongly enhanced by a factor of Q relative to the rate in the absence of the cavity [22]. In all cases, the coupled system shows a transmission dip ($T = 0$) at qubit transition frequency Ω .

By dynamically tuning the transition energy of the two-level system, the transmission of the single photon can be switched on or off. For the single Cooper pair box, the transition energy can be tuned by the magnetic flux through the Josephson junction loop; for quantum dots or hyperfine atomic energy levels, this can be achieved through dc Stark effect. For the single Cooper pair box at the degeneracy point, when E_J is changed to E'_J by varying the magnetic flux, the resonance peak shifts from ω to ω' , as shown in Fig. 4. [Note $\omega(\omega')$ is not equal to $E_J(E'_J)$, due to the coupling with the waveguide propagating modes]. Consequently, an original on resonance photon at frequency ω would become off resonance, as long as the frequency shift is larger than the linewidth of the transmission peak, as shown in Fig. 4(b). If the even sharper Fano resonance peak is employed [Fig. 4(b), inset], the transmission can be switched to any predesigned value with a tiny change in the magnetic field. The SQUID loop area in Ref. [4] is of the order of $1 \mu\text{m}^2$, the change in magnetic field is esti-

mated to be roughly of the order of $0.5 \times \phi_0 / (1 \mu\text{m}^2) \approx 10^{-3}$ T. The switching ability is limited by the modulation speed of the external magnetic field through the SQUID loop. We note that the one-photon switching capability can also be realized by a Mach-Zehnder type interferometer using nonlinear index modulation [23]. The advantage of tuning the transition energy of qubits is the much smaller footprint of the device. It is also possible to achieve the switching via ac pulses with an additional probe gate [8].

As a final remark, we note that this transfer matrix method can deal with different types of cavity walls, such as dielectric slabs, as well. Moreover, it is also straightforward to study the entanglement of multiple qubits via coupling through the one-dimensional continuum [3,6]. By coupling a qubit to a cavity and a one-dimensional waveguide, the transport properties can be manipulated. Furthermore, the Cooper pair box is a class of particularly versatile qubit, for both the physics and the mesoscopic scale allow large tuning capability. We speculate that further clever designs, such as the presence of additional spatial symmetries of the qubits, can be exploited and for sure will bring a much richer content to the field of solid-state realization of quantum computing and quantum information processing devices.

J. T. Shen thanks H.-T. Chou, M. L. Povinelli, J. Shin, and Z. Wang for helpful discussions. Shanhui Fan acknowledges financial support by NSF Grant No. ECS-0134607 and the Packard Foundation.

*Electronic address: shanhui@stanford.edu

- [1] R. J. Thompson *et al.*, Phys. Rev. Lett. **68**, 1132 (1992).
- [2] H. Mabuchi and A. Doherty, Science **298**, 1372 (2002).
- [3] A. Blais *et al.*, Phys. Rev. A **69**, 062320 (2004).
- [4] A. Wallraff *et al.*, Nature (London) **431**, 162 (2004).
- [5] C. Wang *et al.*, Phys. Rev. A **55**, 823 (1997).
- [6] J. T. Shen and S. Fan, Opt. Lett. **30**, 2001 (2005).
- [7] V. Bouchiat *et al.*, Phys. Scr. **T76**, 165 (1998).
- [8] Y. Nakamura *et al.*, Nature (London) **398**, 786 (1999).
- [9] D. Vion *et al.*, Science **296**, 886 (2002).
- [10] Y. Makhlin *et al.*, Rev. Mod. Phys. **73**, 357 (2001).
- [11] R. H. Dicke, Phys. Rev. **93**, 99 (1954).
- [12] P. W. Anderson, Phys. Rev. **124**, 41 (1961).
- [13] P. B. Wiegmann *et al.*, J. Phys. C **16**, 2281 (1983).
- [14] V. I. Rupasov *et al.*, Sov. Phys. JETP **60**, 927 (1984).
- [15] U. Fano, Phys. Rev. **124**, 1866 (1961).
- [16] S. Fan *et al.*, J. Opt. Soc. Am. A **20**, 569 (2003).
- [17] H. A. Haus *et al.*, J. Lightwave Technol. **9**, 754 (1991).
- [18] Y. Xu *et al.*, Phys. Rev. E **62**, 7389 (2000).
- [19] S. Fan, Appl. Phys. Lett. **80**, 908 (2002).
- [20] H. A. Haus, *Waves and Fields in Optoelectronics* (Prentice-Hall, New Jersey, 1984).
- [21] D. M. Pozar, *Microwave Engineering* (John Wiley & Sons, New York, 1997).
- [22] S. Haroche, in *Fundamental Systems in Quantum Optics* edited by J. Dalibard, J. Raimond, and J. Jinn-Justin (Elsevier, New York, 1992).
- [23] M. Soljačić *et al.*, J. Opt. Soc. Am. B **19**, 2052 (2002).